Design of optical/IR blocking filters for the Lynx X-ray Microcalorimeter

Megan E. Eckart
Wonsik Yoon
Benjamin Zeiger
Simon R. Bandler
Dan McCammon

SPIE.

Design of optical/IR blocking filters for the Lynx X-ray Microcalorimeter

Megan E. Eckart,[a,*] Wonsik Yoon,[b] Benjamin Zeiger,[c] Simon R. Bandler,[b] and Dan McCammon[d]

[a]Lawrence Livermore National Laboratory, Livermore, California, United States
[b]NASA Goddard Space Flight Center, Greenbelt, Maryland, United States
[c]Luxel Corporation, Friday Harbor, Washington, United States
[d]University of Wisconsin–Madison, Madison, Wisconsin, United States

Abstract. The Lynx mission concept, under development ahead of the 2020 Astrophysics Decadal Review, includes the Lynx X-ray Microcalorimeter (LXM) as one of its primary instruments. The LXM uses a microcalorimeter array at the focus of a high-throughput soft x-ray telescope to enable high-resolution nondispersive spectroscopy in the soft x-ray waveband (0.2 to 15 keV) with exquisite angular resolution. Similar to other x-ray microcalorimeters, the LXM uses a set of blocking filters mounted within the dewar that pass the photons of interest (x-rays) while attenuating the out-of-band long-wavelength radiation. Such filters have been successfully used on previous orbital and suborbital instruments; however, the Lynx science objectives, which emphasize observations in the soft x-ray band (<1 keV), pose more challenging requirements on the set of LXM blocking filters. We present an introduction to the design of the LXM optical/IR blocking filters and discuss recent advances in filter capability targeted at LXM. In addition, we briefly describe the external filters and the modulated x-ray sources to be used for onboard detector calibration. © The Authors. Published by SPIE under a Creative Commons Attribution 4.0 Unported License. Distribution or reproduction of this work in whole or in part requires full attribution of the original publication, including its DOI. [DOI: 10.1117/1.JATIS.5.2.021020]

Keywords: x-ray spectroscopy; microcalorimeter; detectors; optical blocking filters.

Paper 18103SS received Nov. 2, 2018; accepted for publication May 8, 2019; published online Jun. 11, 2019.

1 Introduction

In x-ray microcalorimeter instruments, the purpose of dewar blocking filters is (1) to shield the detector array from thermal radiation from the instrument and optical and UV photons from the sky and (2) to shield the coldest stages of the instrument from the thermal radiation emanating from the warmer stages. Additional requirements on the filters are to allow x-ray transmission in the scientific band of interest—which has led to the use of thin films—and to be mechanically robust to allow handling, vacuum, and low-temperature operation as well as to withstand launch vibration. Because the x-ray transmission may be drastically reduced by even thin layers of molecular contamination on the filters, we also require that the filter and aperture assembly design minimize the probability of contamination and allow removal of contaminants via filter heaters that can be operated on-orbit. These requirements have led to the use of meshes for mechanical support and to aid in thermal conduction.

Other attenuators in the optical path, which may combine to reduce the total effective area but can also aid in meeting some out-of-band attenuation requirements, include telescope thermal shields, filters on an external-to-the-dewar filter wheel, and the window on the dewar door, the latter of which is typically designed to withstand more than an atmosphere of differential pressure (beryllium is a typical material of choice).

1.1 Heritage

The Astro-H (Hitomi) soft x-ray spectrometer (SXS),[1] launched in 2016, used a series of five thin-film radiation-blocking filters anchored to nested temperature stages that blocked long-wavelength radiation while minimizing x-ray attenuation. The SXS aperture assembly used a system of barriers, baffles, filter carriers, and filter mounts that supported the filters and inhibited their potential contamination. The two inner filters were freestanding with Al/polyimide thicknesses of 50/75 nm. The three outer (warmer) filters were equipped with thermometers and heaters for decontamination and used Al/polyimide thicknesses of 100/100 nm and micromachined silicon support meshes. Further details on the design, implementation, and calibration of the SXS filters and aperture assembly may be found in Refs. 2 and 3. Currently, we are rebuilding the SXS instrument, now named Resolve,[4] for the X-Ray Imaging and Spectroscopy Mission (XRISM),[5] the mission aimed at recovering the calorimeter science lost due to the early loss of the Hitomi satellite.[6] The Resolve filters will be identical to those of SXS. As an example of out-of-band requirements for a microcalorimeter instrument, for Resolve, the required maximum out-of-band transmission of each of the thinner freestanding filters is 5×10^{-3} in the visible and 5×10^{-4} in the IR range (3 to 25 μm), of each of the thicker mesh-supported filters is 5×10^{-5} in the visible and 1×10^{-4} in the IR and of the combination of the filters and telescope thermal shield is 1×10^{-4} at 40.8 eV (geo-coronal He II), 2×10^{-5} at 21.2 eV, and 1×10^{-6} at 10.2 eV.

The SXS filters built on designs developed for the X-ray Quantum Calorimeter (XQC) sounding rocket experiment,[7,8] which has flown six times and used even thinner thin-film layers than SXS, with nominal thicknesses of ~25-nm Al and 50-nm polyimide. Similar filters also flew on the Micro-X Sounding Rocket experiment in 2018.[9]

The X-ray Integral Field Unit (X-IFU)[10,11] on the Athena x-ray observatory, scheduled for launch in 2031, will use ~3000 transition-edge-sensor microcalorimeters. The X-IFU

*Address all correspondence to Megan E. Eckart, E-mail: eckart2@llnl.gov

will also use a set of optical blocking filters, and these are currently under development. While the basic design will be similar to those developed for previous microcalorimeter missions, the X-IFU filters team is exploring several options, including meshes of different material than silicon and replacing the thin film to use SiN instead of polyimide.[12,13] One interesting option currently under consideration for the X-IFU is to coat the microcalorimeter pixels with a thin layer of Au to increase the reflectivity in the optical and IR. The pixels under development for the X-IFU use Au/Bi absorbers, where the material facing the telescope is Bi, which has lower reflectivity in the optical and IR compared to the Au/Bi/Au stack under consideration. Increasing the reflectivity of the microcalorimeter x-ray absorbers means that the out-of-band transmission requirements of the filters will be relaxed.

1.2 Considerations (Differences) for Lynx X-ray Microcalorimeter

Although the Lynx filters will retain heritage based on the previous missions, there are a few important differences that will drive aspects of the design.

1. Science drivers. The Lynx science objectives have more of a focus on the low-energy (<1 keV) part of the bandpass compared to SXS and the X-IFU, which drive us to designs that have thinner films, or even to consider filters that use attenuation methods other than reflection by thin films. Some requirements may be fulfilled by adding an additional optical blocking filter on the external filter assembly that would be inserted for observations of bright sources, reducing the requirements on the dewar blocking filters.

2. X-ray absorbers. The x-ray absorbers used for the Lynx X-ray Microcalorimeter (LXM) array will be made of Au, which, as in the case of the X-IFU detectors coated with Au (see Sec. 1.1), will relax the requirements on the out-of-band transmission. The pure Au reflection is >98% at wavelengths above 1 μm.
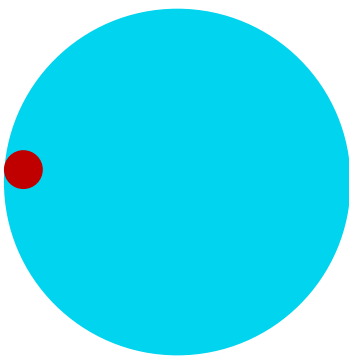

Fig. 1 Comparison of the smallest filter needed for the LXM extended array option (89-mm diameter; blue) compared to that of the Astro-H SXS (10-mm diameter; red), emphasizing the step change in filter technologies required for the extended focal plane. Larger filters increase challenges of uniformity and mechanical stability. The smallest filter in the baseline LXM design is 26 mm (see Fig. 2), much closer to the current state of the art.

3. Size of the aperture. The baseline size for the LXM detector array is slated to be 22 mm: larger than that of Astro-H and XRISM but similar to that of Athena X-IFU. If the extended array option[14] is employed for LXM, which uses a 60-mm detector array, then the filters will be significantly larger than those of X-IFU as well (see Fig. 1).

4. Orbit. Lynx will reside at L2, unlike Astro-H and XRISM, which use low Earth orbits. At L2, the 40.8-eV geocoronal line is much fainter, and thus not such a driver of the out-of-band transmission requirements.

2 Lynx X-ray Microcalorimeter Optical Blocking Filter Design

For the LXM baseline design, we have chosen to use six filters, four of which are "conventional," with thin aluminized polyimide films supported by silicon meshes, and two of which are waveguide-cutoff filters that do not employ thin films. The driving factor behind this choice is the need for a higher transmission at low x-ray energies. Table 1 summarizes the baseline LXM filter stack in comparison to previous missions. The waveguide-cutoff filters reduce the x-ray transmission by a geometrical factor set by the mesh parameters, but because the holes are open, and not covered by a film, the transmission through the holes is unity across the x-ray waveband. For the conventional filters, we have chosen thinner films, again to increase the soft-band x-ray transmission. Each filter will be ~10-nm Al/20-nm polyimide. We expect the out-of-band long-wavelength attenuation of these thin filters will be limited by the few nm-thick oxide on each filter.[15] Fabrication experts are working to study representative thin films and the resulting effects of the oxidation (see Sec. 3). The baseline films are thinner than those used for previous missions, and if we cannot meet the out-of-band rejection requirements or if they are too fragile (i.e., cannot survive handling or environmental tests with high reliability) we can employ thicker films, as described below.

2.1 Need for Support Meshes

For large filters, and with the typical thin-film materials, support meshes are required even though they reduce the filter transmission. Figure 2 provides an example of the silicon support meshes used for Astro-H SXS. When filters are small enough, we may omit the mesh. But, unlike the case of SXS and Resolve, meshless filters are impractical for the Lynx microcalorimeter instrument for even the smallest filters. This statement holds for all filters in the current Lynx baseline design (even without the extended array). The size of the LXM detector array means that the dewar filters will be large (a few cm diameter), and thin, freestanding films with this diameter will be too fragile. For Astro-H, the largest freestanding filter was 12-mm diameter. The 18.5-mm-diameter filter and larger required a mesh for mechanical support. The baseline Lynx design has the smallest (coldest) Lynx filter at 26-mm diameter for the baseline array configuration. And, the proposed Lynx films are thinner (more fragile) than the Astro-H filters. We conclude that based on technology demonstrations to date, the baseline Lynx design should have meshes for all filters.

Table 1 Summary of dewar blocking filters for heritage instruments and LXM. For both X-IFU and LXM, the size of the aperture requires all filters to have mechanical support meshes.

Mission	Instrument	Launch year	No. of filters	No. of meshes	Film thicknesses	
					Total Al (nm)	Total polyimide (nm)
Sounding rocket	XQC	Multiple	6	4	120	270
Astro-H	SXS	2016	5	3	385	488
XRISM	Resolve	2022	5	3	400	450
Athena	X-IFU	2031	5	5	150	225
Lynx	LXM	mid-2030s	6	6[a]	40	80

[a]For LXM two of the six filters are assumed to be waveguide-cutoff filters: they are counted as a filter with a mesh but they do not have thin films, and thus do not contribute to the tabulated Al or polyimide thicknesses.

(a)
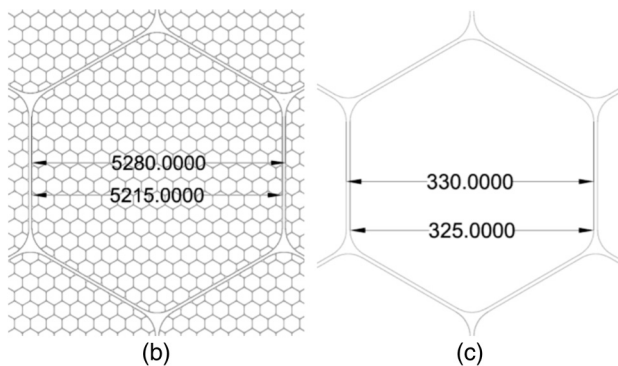
(b)   (c)

Fig. 2 (a) Example of a silicon support mesh sitting in an aluminum fixture, photographed before the application of the thin film. The coarse hexagonal mesh is easily visible; the fine mesh is visible within each coarse mesh hexagon. Dimensions (in microns) of the (b) coarse mesh and (c) fine mesh of the three mesh filters used for Astro-H SXS. The coarse mesh bar width is 65 μm and the fine mesh bar width is 5 μm. This panel is adapted from Ref. 2.

Fig. 3 X-ray transmission for the baseline LXM optical/IR blocking filter stack. The transmission at low energies is limited by the aluminized polyimide. The transmission at higher energies increases as the Si support meshes become transmissive. The edge at 12 keV comes from the waveguide-cutoff filters that we assume are made of Au. The broadband mass attenuation coefficients are from Ref. 16. The C, N, and O edge structure is modeled based upon measurements of Astro-H SXS filters.[3] Detailed Al and Si edge structure is not included in this plot.

2.2 Rationale for Proposed Filter Composition and Resulting X-Ray Transmission

We assume six filters, with support meshes on all filters. The total film thickness is 40-nm Al/80-nm polyimide, assumed to be split over 3 to 4 filters. These are quite thin films if split over four filters and moderately thin if on three filters. Waveguide-cutoff filters (no film) are assumed for 2 to 3 of the filters. See Sec. 3 for information about the waveguide-cutoff filters.

The transmission of this set of filters is shown in Fig. 3, and comparisons to Astro-H SXS and Athena X-IFU are presented
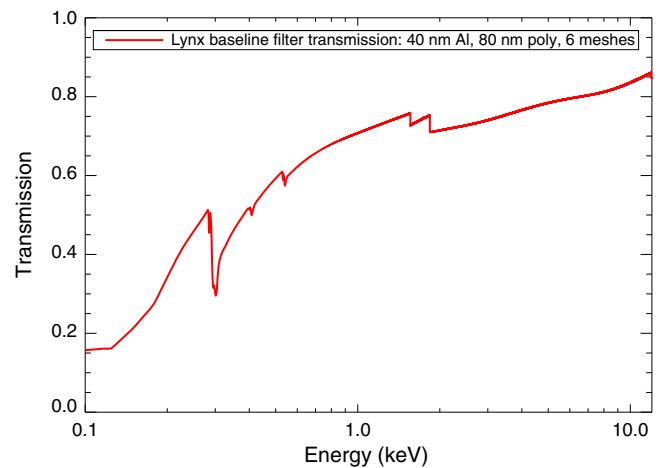
in Figs. 4 and 5. In this calculation, we assume the Athena support meshes are thick metal meshes with 2% blocking factor[13] and Lynx support meshes are identical to the mesh of the Astro-H SXS dewar main shell filter, with 97.5% open-area coarse Si mesh (208-μm Si) plus 97.5% open-area fine mesh (8-μm Si). We assume that the waveguide-cutoff filters for Lynx have the same geometry as the Astro-H meshes, including a thick coarse mesh and a thinner fine mesh but are made of Au. For the "mesh Lynx" curves in Figs. 3–5, we assume two waveguide-cutoff filters, indicated by the larger number of meshes than films.

A cross-sectional diagram of the filters in the LXM dewar is presented in Fig. 6 and details about the implementation, including the filter locations, temperatures, and sizes, are presented in Table 2.

The smallest LXM filter is similar to the size of the Astro-H SXS mesh filters, and the larger LXM filters are in-family with the size of the Athena X-IFU filters, which are currently under development.[12,13] While we have baselined Si meshes similar to
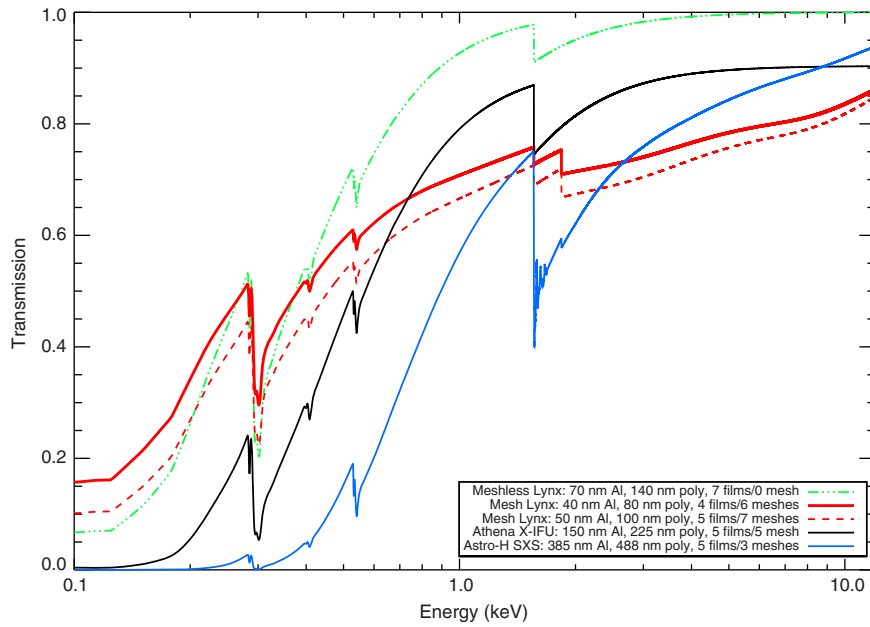
Fig. 4 X-ray transmission for representative LXM filter stacks compared to Athena and Astro-H microcalorimeter instruments. In this plot, we show the filter transmission from 0.1 to 12 keV in lin-log space. For Lynx, we include a curve showing the baseline configuration (4 films/6 meshes) as well as a more conservative option where seven filters are in use (5 films/7 meshes). In addition, we include a physically impractical "meshless" Lynx example, to illustrate the trend if we were to implement a stack of seven freestanding thin-film filters. The broadband mass attenuation coefficients are from Ref. [16]. The C, N, and O edge structure is modeled based upon measurements of Astro-H SXS filters.[3] Detailed Al and Si edge structure is included for the Astro-H curve[3] but is not included in the Lynx or Athena curves in these plots. At low energies, the Lynx filters are the most transmissive, followed by the Athena filters then the Astro-H filters due to the total film thickness used for each instrument. Conversely, at high energies, the Astro-H SXS transmission is the highest due to it using the fewest number of filter meshes, followed by Athena X-IFU and then Lynx. The Athena X-IFU curve is flatter at high energies because the current X-IFU baseline has thick metal meshes, not a combination of thick and thin (coarse and fine) meshes as in the case of Astro-H and Lynx.
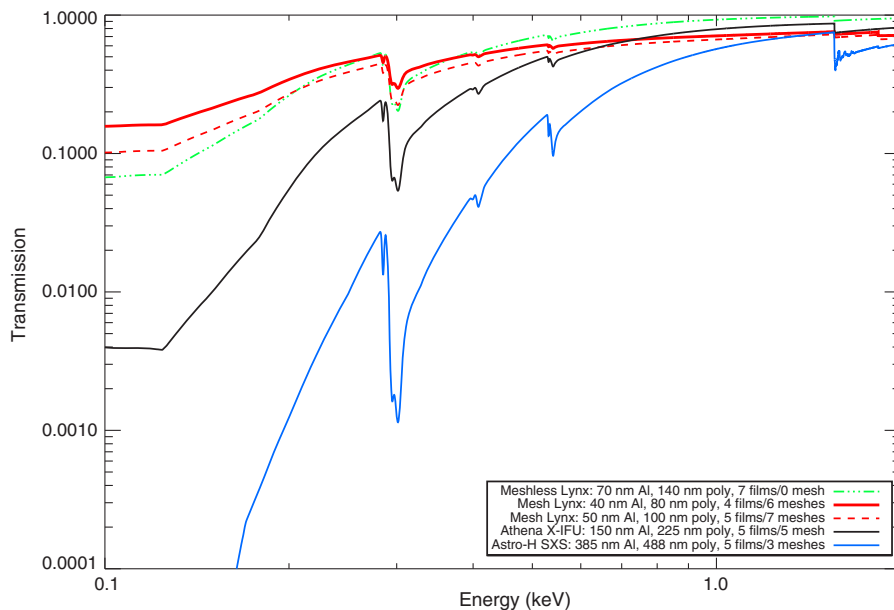

Fig. 5 X-ray transmission for representative LXM filter stacks compared to Athena and Astro-H microcalorimeter instruments. This panel is plotted on a log–log scale and highlights the low-energy portion of the bandpass. The Lynx filter stack provides an increase of 2 orders of magnitude at 0.2 keV compared to the Astro-H SXS. See Fig. 4 caption for explanations of each curve.
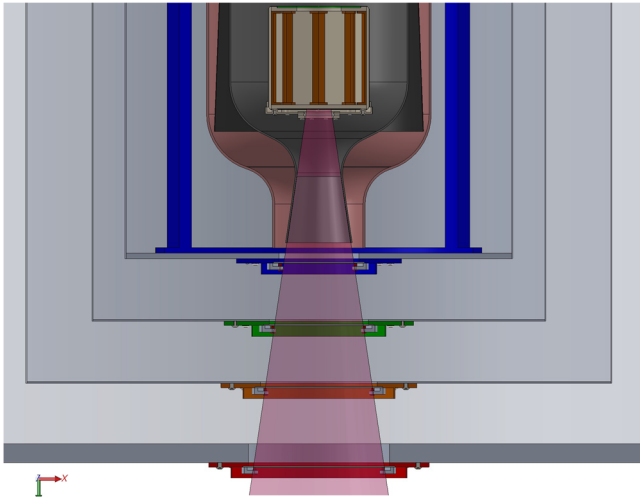
Fig. 6 Solid model of the LXM dewar, showing a cross section of the dewar optical blocking filters. The smallest (coldest) filter is mounted to the top of the focal plane assembly, shown near the top of the figure. The other filters are marked in blue, green, orange, and red. The expected beam from the telescope is illustrated in pink. Table 2 lists the size and other details of these filters. The clear aperture of each filter takes into account the expected beam size from the telescope plus margin for alignment and for illumination by the modulated x-ray sources (MXSs) (see Fig. 9).

regarding mesh and filter design and fabrication. We do not anticipate a reduction in fabrication yield of the films themselves for the LXM filters compared to filters with smaller diameters.

The final filter composition and transmission may change as follows:

- If more transmissive support meshes are developed (of Al, plastic, etc.), the overall transmission will rise, and the high energy (>1 keV) transmission will be closer to unity, improving the instrument performance. Development work on mesh materials is ongoing, but for use on LXM, there will need to be an improvement in strength of these alternate meshes.

- If new filter films are developed that are stronger (e.g., use of a more robust plastic in place of polyimide), we may not require meshes on all filters and the overall transmission will rise, improving the instrument performance. As with mesh materials, we have baselined LXM filters that use thin-film materials with significant flight heritage rather than relying on advances that are currently under development.

- If the proposed Al thickness is too thin to meet the optical/IR blocking requirements, we will need thicker filters and the transmission at low energies will drop. This is one of the biggest uncertainties in the predicted filter transmission curves, as the baseline design includes filters that are significantly thinner than previously flown.

- If the waveguide-cutoff filters do not work as predicted, we may need additional films and the transmission at low energies will drop.

- We do not yet have robust out-of-band (UV/optical/IR) transmission requirements for LXM, although we do plan to develop them in the coming months. Because LXM's Au absorbers are more reflective than those on other microcalorimeter instruments (Astro-H, XRISM, and Athena baseline array), some of the out-of-band requirements may be relaxed, leading to the possibility of thinner filters, which would cause the transmission to increase.

those of Astro-H SXS, the mechanical properties of such meshes at larger sizes will need to be studied in detail. This mechanical analysis has not yet been performed. A change in the mesh design may be required to change the resonance frequencies or quality factors, which could involve selectively thickening the bars. Studies of the mesh fabrication yield will also be performed, and, if the yield is not high enough for large Si meshes, then alternate mesh materials will be adopted. In addition to mechanical mesh failures, defects in the mesh or adhesive that bonds the mesh to the thin film can lead to filter film failures during environmental testing, in particular for the thin films baselined for LXM, so this will also be studied for Lynx and is currently under study for Athena X-IFU. We will incorporate any lessons learned from the X-IFU development program

Table 2 Left columns: dewar filter thermal interface, filter abbreviation, nominal operating temperature, clear aperture diameter, expected beam diameter from the telescope, and distance from the filter to the detector. The larger diameter of the clear aperture compared to the expected beam diameter provides alignment margin and allows greater illumination by the MXSs. Right columns: baseline thin-film component thicknesses.

Interface	Filter abbreviation	Nominal temperature (K)	Clear aperture (mm)	Beam size (mm)	Height (mm)	Film thicknesses	
						Al (nm)	Polyimide (nm)
Focal plane assembly	FPA	0.050	26	23.5	5	10	20
4K Shield # 1	4K_1	4	72.5	62.5	139	10	20
4K Shield # 2	4K_2	4	a	a	a	n.a.	n.a.
15K Shield	15K	15	90	80	195	n.a.	n.a.
80K Shield	80K	80	106	96	252	10	20
Dewar main shell	DMS	285	128	118	324	10	20

[a]Denotes that the waveguide-cutoff filter mesh at 4K (that does not use a thin film) is not shown in Fig. 6, and exact filter dimensions are not specified. The filter will likely be a few mm farther from the detector than filter 4K_1, with a similar clear aperture diameter.

3 Technology Development and Testing for Lynx X-ray Microcalorimeter Optical Blocking Filters

Several areas of technology development have been pursued to provide enhanced options for the LXM optical blocking filters. In this section, we present an overview of some of these studies, each of which will be explained in more detail in upcoming articles.[17,18]

The Luxel Corporation has undertaken several studies of thin-film filters for LXM. Similar to studies underway for Athena X-IFU filters, they have been exploring the possibility of using silicon nitride instead of polyimide to provide an increase in low-energy transmission. Figure 7 shows an example of the increase in transmission at energies below 100 eV offered by exchanging a 200-nm polyimide film for a SiN film of half the thickness.

Luxel has also been studying the reflectance and absorption of thin aluminized polyimide films in the optical, NIR, and FIR. They measured samples of various aluminum thicknesses, into the regime where the aluminum becomes thinner than their standard products ($\lesssim$25 nm) and approaches the thicknesses specified for LXM. Figure 8 presents initial results of measurements on films with aluminum thicknesses ranging from 12 to 33 nm. The value of the initial reflective surface even in very thin coatings is apparent in Fig. 8. For example, two 12-nm Al films will have lower IR transmission than a single 24-nm Al film for wavelengths >1 μm. While x-ray transmission will not be identical for these scenarios due to the native oxide layer on the Al surfaces, the data show that the optical blocking per unit thickness is improved with thinner Al films. The 1-μm data do not follow this trend, indicating that the shorter wavelengths may be passing through discontinuities in the thin Al surface whereas longer wavelengths can span the discontinuities and see a more continuous surface. The data may suggest that thinner Al layers are particularly viable deeper in the Lynx filter stack to block infrared photons from warmer stages, whereas outer filters should maintain an optically continuous layer of >25 nm to attenuate shorter wavelengths. Fabrication procedures that provide more continuous thin Al films are under investigation.

In addition, to test whether extreme ultraviolet (EUV) radiation would increase the aluminum oxidation on-orbit and thus lessen the optical/IR attenuation, Luxel worked with partners at the National Institute for Standards and Technology (NIST), Gaithersburg, Maryland, and the Laboratory for Atmospheric
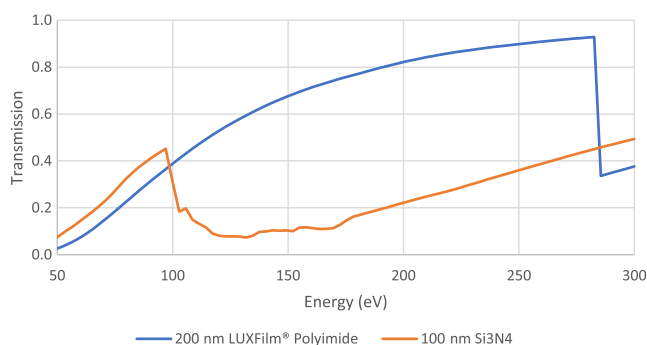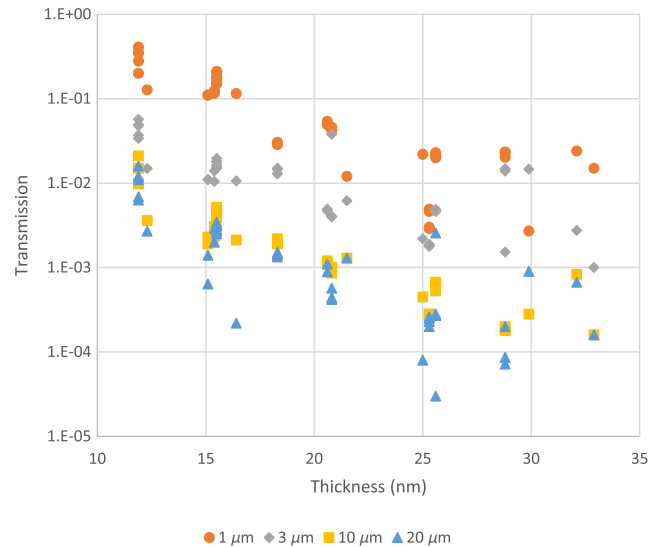
Fig. 8 Measured transmission of Luxel Al/polyimide filters as a function of Al thickness at wavelengths from 1 to 20 μm. The transmission is affected by both reflection and internal absorption. The thickness accuracy is 1.5 nm and the transmission measurement accuracy is of order 10^{-4}. The quoted Al thicknesses are not corrected for oxidation (they include the Al and the oxide layers) and were measured via a KLA model P-7 contact profilometer on a witness sample adjacent to the film during deposition.

and Space Physics to irradiate aluminized polyimide filters with EUV photons using the SURF-III facility at NIST. Some filters did exhibit increased oxidation; however, it was clear that while this effect must be considered for missions that will experience intense solar EUV radiation, this will not be a problem for the much lower intensity levels that Lynx will experience. Additional details will be available in a forthcoming paper.[17]

In addition to these studies of advanced thin-film filters, several groups (e.g., groups led by R. Fettig, D. McCammon, and E. Wollack) have been exploring the feasibility of using waveguide-cutoff filters to block long-wavelength radiation using a periodic array of hexagonal holes with thin walls. This configuration should result in a far-infrared cutoff frequency where the hole size is used to control the onset of the high-pass response and thickness determines the rejection. These filters have heritage in metal mesh filters that have been used for many years in the sub-mm and mm astronomy communities. Advances in experimental realizations of these filters will be described in Ref. 18, an upcoming paper from researchers in both the US and Germany and from both the Lynx and Origins Space Telescope study teams. The geometries that have been explored by various groups include meshes of different materials and different length-to-width ratios of the holes. The x-ray blocking fraction of recent designs is similar to that of the Si support meshes used for Astro-H SXS, although preliminary testing showed a slight increase in x-ray blocking fraction due to details of the filter fabrication.

Fig. 7 Comparison of transmission of 100-nm silicon nitride to that of 200-nm-thick LUXFilm polyimide in the low-energy x-ray bandpass, calculated using literature values of the mass absorption coefficients.[16] The polyimide density is 40% that of silicon nitride.

4 Filter Wheel and Modulated X-Ray Sources

Figures 9 and 10 present views of the dewar model highlighting the current design of the LXM filters (external to the dewar) and MXSs.
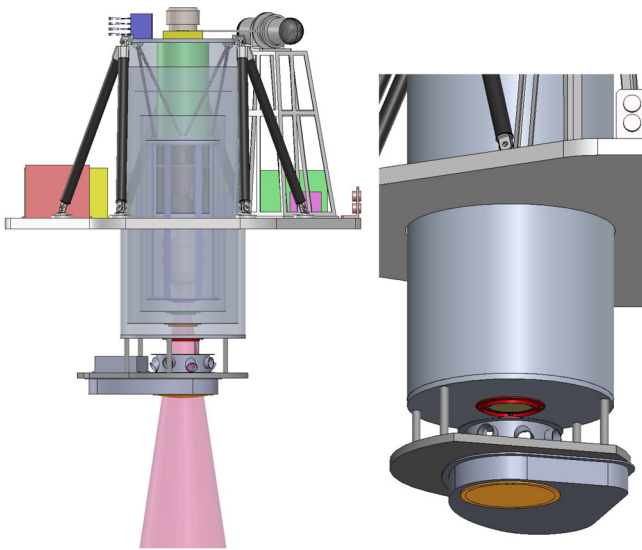
Fig. 9 Dewar model drawings highlighting the LXM external filter assembly and mounting location for the MXSs. The dewar gate valve (door) is not shown in these figures. The diameter of the ring holding the MXSs will be smaller than what is shown in figure to allow greater coverage of the detector array by each MXS without having to make the dewar blocking filters significantly larger.
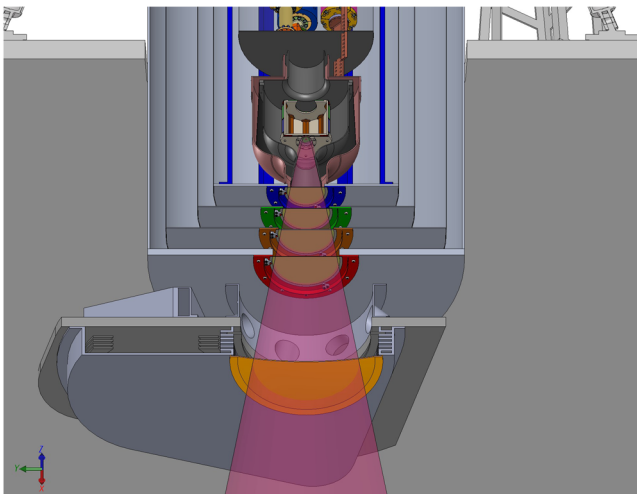

Fig. 10 Dewar model cross section highlighting the LXM external filter mounting scheme. To avoid a large diameter wheel, the LXM filters are mounted on paddles that are stacked vertically on top of one another so that one (or more) filter can swing into the optical path and housed in the gray assembly at the bottom of the figure. The dewar gate valve (door) is not shown in this figure.

To avoid a large diameter wheel, the LXM filters are mounted on paddles that are stacked vertically on top of one another so that one (or more) filter can swing into the optical path. The filters are housed in the gray module shown in the bottom of the right panel of Fig. 9. The optical path is highlighted by the orange circle on the filter assembly. At the current level of development, we assume filters similar to those used for Astro-H SXS,[19] including Be filters to reduce the low-energy flux and a neutral density filter to provide an energy-independent reduction in flux. For LXM, we plan to use an aluminized polyimide optical blocking filter instead of the polyimide-only contamination blocking filter on Astro-H, to add margin in the

event that one of the dewar filters is damaged or degrades. This change will be implemented for XRISM Resolve as well. LXM will have a suite of eight MXSs for calibration of the detector gain, real-time monitoring of the gain drift, and measurements of the core line-spread function (energy resolution). The MXSs themselves are not shown in the model, but their mounting fixtures are apparent in the ring mounted between the dewar entrance and the external filter assembly. The MXSs are assumed to be similar to the ones used for Astro-H SXS[19] and Athena X-IFU.[20] For Astro-H SXS, there were two MXSs with "direct" illumination that could be used for gain drift monitoring and two "indirect" fluorescent sources that provided low-energy lines but were dim enough that they could only be used at high duty cycles (~50%). In Fig. 9, the mounting spaces for the direct MXSs are shown as tubes pointing diagonally toward the detector. The indirect sources would be mounted parallel to the ring pointing at a fluorescent target. Other implementations may be possible as there are development efforts underway to build brighter MXSs that provide low-energy lines. In the case of Astro-H SXS, only one MXS was operated at a time and each MXS illuminated the entire detector array. This configuration meant that it was the sightline of the MXS that drove the requirements on the size of each filter clear aperture. For LXM, we plan to operate more than one MXS at a time to illuminate the entire detector array; with the current design, each MXS will only illuminate approximately half of the detector array.

5 Conclusion

We have presented the baseline design of the LXM optical blocking filters and compared the filters to those on recent and upcoming microcalorimeter instruments, such as the Astro-H SXS and Athena X-IFU. The LXM will aim to provide a higher filter transmission at low energies than the previous missions, which leads to the use of very thin Al/polyimide filters and waveguide-cutoff filters. The size of the LXM detector array, in the baseline configuration, means that the blocking filters will be of a spatial extent large enough that they will need mechanical support meshes (given technical demonstrations to-date) but are in-family with the size of filters required for the Athena X-IFU. If the extended array option is chosen, then significantly larger filters will be required and additional care will be needed to be taken with regard to mechanical properties and uniformity. We have briefly introduced a few of the filter testing and technology development projects underway to address the LXM filter baseline design and enhanced goals, including studies of filters with thin Al layers and of waveguide-cutoff filters using arrays of hexagonal holes. We find that fabricating films consistent with the LXM baseline design that meet the out-of-band blocking requirements will be challenging and need to be verified during the Lynx development program; the filters may need slightly thicker Al. We have also presented the basic configuration of the filters and MXSs mounted outside of the LXM dewar.

References

1. R. L. Kelley et al., "The Astro-H high resolution soft x-ray spectrometer," *Proc SPIE* **9905**, 99050V (2016).

2. C. A. Kilbourne et al., "Design, implementation, and performance of the Astro-H soft x-ray spectrometer aperture assembly and blocking filters," *J. Astron. Telesc. Instrum. Syst.* **4**, 011215 (2018).

3. M. E. Eckart et al., "Ground calibration of the Astro-H (Hitomi) soft x-ray spectrometer," *J. Astron. Telesc. Instrum. Syst.* **4**, 021406 (2018).

4. Y. Ishisaki et al., "Resolve Instrument on X-ray Astronomy Recovery Mission (XARM)," *J. Low Temp. Phys.* **193**, 991–995 (2018).

5. M. Tashiro et al., "Concept of the X-ray Astronomy Recovery Mission," *Proc SPIE* **10699**, 1069922 (2018).

6. T. Takahashi et al., "Hitomi (ASTRO-H) X-ray Astronomy Satellite," *J. Astron. Telesc. Instrum. Syst.* **4**, 021402 (2018).

7. D. McCammon et al., "A high spectral resolution observation of the soft x-ray diffuse background with thermal detectors," *Astrophys. J.* **576**, 188–203 (2002).

8. S. G. Crowder et al., "Observed limits on charge exchange contributions to the diffuse x-ray background," *Astrophys. J.* **758**, 143 (2012).

9. P. Wikus et al., "Progress on the Micro-X Sounding Rocket X-Ray Telescope: completion of flight hardware," *Proc. SPIE* **7732**, 77321P (2010).

10. D. Barret et al., "The ATHENA X-ray Integral Field Unit (X-IFU)," *Proc. SPIE* **10699**, 106991G (2018).

11. F. Pajot et al., "The Athena X-ray Integral Field Unit (X-IFU)," *J. Low Temp. Phys.* **193**, 901–907 (2018).

12. M. Barbera et al., "Baseline design of the thermal blocking filters for the X-IFU detector on board ATHENA," *Proc. SPIE* **9144**, 91445U (2014).

13. M. Barbera et al., "ATHENA X-IFU thermal filters development status toward the end of the instrument phase-A," *Proc. SPIE* **10699**, 106991R (2018).

14. S. R. Bandler et al., "The Lynx x-ray microcalorimeter—LXM.," *J. Astron. Telesc. Instrum. Syst.* accepted (2019).

15. L. Sciortino et al., "Surface investigation and aluminum oxide estimation on test filters for the ATHENA X-IFU and WFI detectors," *Proc SPIE* **9905**, 990566 (2016).

16. B. L. Henke, E. M. Gullikson, and J. C. Davis, "X-ray interactions: photoabsorption, scattering, transmission, and reflection at E = 50–30, 000 eV, Z = 1–92," *At. Data Nucl. Data Tables* **54**, 181–342 (1993).

17. B. Zeiger, H. Lopez, and T. Ayers, "Advances in optical blocking filters for the Lynx x-ray microcalorimeter," in preparation (2019).

18. E. Wollack et al., "Technology development of advanced filter design for the Lynx x-ray microcalorimeter," in preparation (2019).

19. C. P. de Vries et al., "Calibration sources and filters of the soft x-ray spectrometer instrument on the Hitomi spacecraft," *J. Astron. Telesc. Instrum. Syst.* **4**, 011204 (2018).

20. C. P. de Vries et al., "Simulating modulated x-ray calibration sources for future x-ray missions using GEANT4," *Proc. SPIE* **10699**, 1069965 (2018).

Megan E. Eckart is a research scientist in the Astrophysics and Advanced Diagnostics Group at the Lawrence Livermore National Laboratory.

Wonsik Yoon is a researcher in the Detector Systems Branch at NASA's Goddard Space Flight Center.

Benjamin Zeiger is the Chief Scientist of Luxel Corporation.

Simon R. Bandler is a research astrophysicist in the X-ray Astrophysics Group at NASA's Goddard Space Flight Center.

Dan McCammon is a professor in the Physics Department at University of Wisconsin–Madison.